Samuel I. Outcalt, Kenneth M. Hinkel

Erika Meyer, and Anthony J. Brazel

Application of Hurst Rescaling to Geophysical Serial Data

The empirical investigation of several geophysical time series indicates that they are composed of segments representing different natural regimes, or periods when events are strongly autocorrelated. Using a data transformation method developed by Hurst, these regimes are differentiated by rescaling the time series and examining the resulting transformed trace for inflections. As regime signals are not completely mixed and have rather long run lengths, Hurst rescaling produces a clustering of extremes of the same sign and elevates the Hurst exponent to values greater than 0.5. These regimes have a characteristic distribution, as defined by the mean and standard deviation, which differ from the statistical characteristics of the complete record. Analysis of sunspot numbers, monthly precipitation records from the midwestern United States, and annual watershed discharge yield regimes that correlate to well-documented periods of extreme activity. Rescaling appears to be useful in screening time series of unknown characteristics to differentiate periods dominated by regime-specific physical processes.

INTRODUCTION

The methods developed by Hurst (1951) to study the discharge of the Nile and other geophysical serial data are now recognized as pioneer explorations in natural fractal geometry (Mandelbrot 1982). Using historical records, Hurst was attempting to estimate the reservoir storage required to contain the Nile floodwater. To this end, he employed a technique of time-series transformation, referred to here as *Hurst rescaling*.

Hurst rescaling entails subtracting the mean of the series from each of the n observations in the record. These deviations from the mean are accumulated to

Samuel I. Outcalt is adjunct professor emeritus, Kenneth M. Hinkel is associate professor, and Erika Meyer is a graduate student in the department of geography at the University of Cincinnati. Anthony J. Brazel is professor of geography at Arizona State University.

form a transformed series R. The *adjusted range* $R(n)$ of the series is equal to $(R_{max} - R_{min})$.

The adjusted range, divided by the standard deviation (S) of the record, yields the *rescaled range*. The rescaled range is expected to increase asymptotically with the square root of the number of record observations (n). The exponent H, with an anticipated value of 0.5, is termed the *Hurst exponent* (Schroeder 1991). These relationships are shown as equation (1).

$$[R(n)/S(n)] \propto n^H. \tag{1}$$

The value of H is crudely calculated as the log of the rescaled range divided by the number of observations, as shown in equation (2).

$$H = \log[R(n)/S(n)]/\log n. \tag{2}$$

This form of equation (2) is used by Schroeder (1991, p. 130), and described as "a convenient measure of the persistence of a statistical phenomena." It is employed here rather than the form favored by Potter (1979), in which the denominator is log (n/s).

Through empirical observation, Hurst and others recognized that, for many geophysical time series, the value of H is greater than 0.5 and frequently ranges from 0.6–0.9 (Hurst, Black, and Simaika 1965; Church 1980). This effect has been termed the *Hurst phenomenon*. Interpretations of the Hurst phenomenon have been abundant in the geophysical literature. Mandelbrot and Wallis (1969) and Mandelbrot (1982) attribute the nonrandom behavior of river discharge to "persistence," which is the temporal grouping of nonperiodic, similar events. Furthermore, they associate Hurst exponent values with fractional noises. The Hurst exponent can range from *brown noise* $(H = 0.5)$ for a series with little persistence, through *black noise* $(H = 1.0)$ which characterizes extreme persistence. A value of H near 0.5 therefore indicates chaotic effects due to weak information storage capacity, and this is observed as an absence of long-term temporal correlations (Stolum 1996).

Klemes (1974), however, states that the heightened persistence of the Hurst phenomenon may be the result of a nonstationary, or shifting, record mean. He also claims that H values can be affected by characteristics of the stream storage system, and therefore asserts that a physical, rather than a mathematical, model of the effect would be extremely useful. Potter (1976, 1979), Church (1980), and Mesa and Poveda (1993) also attribute the Hurst phenomenon to a nonstationary mean. Conversely, Wallis and O'Connell (1973) suggest that the Hurst phenomenon can be explained with a mixed autoregressive-moving average model. Boes and Salas (1978) demonstrate that the nonstationary model is but a special case of the mixture model, as they have the same correlation structure and generate similar pox diagrams. Thus, it is generally believed that elevated values of H result from pooling samples with different distribution characteristics.

This study will concentrate on the fundamental aspect used by Hurst and others—the rescaling transformation. In particular, we will demonstrate the power of Hurst rescaling in screening serial data for regime transitions. These occur at significant rescaled trace inflections, which signal the boundary of time-series segments characterized by statistical properties differing from the complete time series. The regimes that are defined by Hurst rescaling presumably reflect the effects of changes in the forcing mechanisms for a major duration. In the examination of geophysical serial data, investigators frequently use arbitrary time divisions, such as decades of mean annual values, to test for significant

changes using statistical parameters. Hurst rescaling liberates investigators from using arbitrary periods or the informal method of "visual decomposition."

To achieve our goal, a simple nonstationary model will be employed that appears to be validated by the empirical data. Our general model is similar to that of Potter (1976), who initially attributed the Hurst phenomenon to regimes with different statistical distributions but later ascribed to "acquisition artifacts" effects; in this case, the movement of the weather station or stream gaging site (Potter 1979).

A CONCEPTUAL MODEL OF THE HURST EFFECT

Suppose that one measured the diameters of trees found in three distinct zones along a transect. These zones could represent ecotones characterized by a differing dominant tree species, or could characterize regions in varying stages of vegetation succession. The diameter of each tree is recorded as a sequence by zone, as shown in Table 1. In this example, ten trees from each of the three zones yields a series of thirty observations. The maximum, minimum, mean, and standard deviation for each zone and the pooled sample are also reported.

Hurst rescaling entails accumulating deviations of the observation values from the pooled mean. For example, observation 1 has a circumference of 19.7 centimeters, which is 2.98 centimeters less than the pooled mean (22.68) as shown in the third column of Table 1. Observation 2 is 2.88 centimeters smaller than the pooled mean, and this deviation is added to the running sum to obtain −5.87.

Deviations from the pooled mean are thus calculated and accumulated for the entire series. Minimum and maximum deviations are used to calculate the adjusted range: in this case 33.683. As discussed earlier, the rescaled range is the adjusted range divided by the pooled standard deviation (33.683/2.586). Thus, from equation (2), H is 0.762 for the entire series, which suggests long-term persistence.

The advantage of rescaling is illustrated in Figure 1. Here, the observations are graphed as a series. In this and subsequent figures, all measurements and their transforms have been normalized to a range of 0.0 to 1.0. To normalize the tree diameters (column 5), for example, the minimum observed value of 19.3 is subtracted from each observation, and the remainder is divided by the sample range (7.9). In a similar manner, the rescaled sum in normalized by using the adjusted range of the rescaled series (−33.683), as shown in column 4. The sample and pooled means are calculated in the same way.

Normalization is performed for two purposes: (1) it allows the raw and rescaled data to be displayed on the same diagram, and (2) normalization has no impact on the trace pattern or the estimate of H. For example, we could have first normalized the tree diameter data without affecting either H or the trace.

The primary advantage lies in the ease in interpreting the rescaled series. In Figure 1, it is clear that the Zone 1 average (20.07) is well below the pooled mean of 22.68. Thus, deviations are negative and accumulated deviations yield a trace with a negative slope for observations 1–10. A descending trace therefore indicates persistence of lower-than-normal observations.

A significant trace inflection occurs near the zonal boundary at observation 10. Several of the Zone 2 trees have diameters approaching the pooled mean, yielding a trace with a slope near zero. Because most of the observations in Zone 2 are well below the pooled average, the overall slope is negative and the trace reaches a global normalized rescaled minimum value of 0.0 near the zonal boundary.

TABLE 1
Raw, Accumulated Deviations, and Normalized Data for Individual, Zonal, and Pooled Tree
Diameters

1	2	3	4	5
Observation	Diameter (cm)	Accumulated Deviations from mean (R)	Accumulated Normalized Deviation	Normalized Diameter
		Zone 1		
1	19.7	−2.983	0.911	0.051
2	19.8	−5.867	0.826	0.063
3	19.3	−9.250	0.725	0.000
4	21.0	−10.933	0.675	0.215
5	20.0	−13.617	0.596	0.089
6	20.0	−16.300	0.516	0.089
7	20.5	−18.483	0.451	0.152
8	20.8	−20.367	0.395	0.190
9	20.2	−22.850	0.322	0.114
10	19.4	−26.133	0.224	0.013
		Zone 2		
11	22.8	−26.017	0.228	0.443
12	22.5	−26.200	0.222	0.405
13	22.0	−26.883	0.202	0.342
14	23.0	−26.567	0.211	0.468
15	21.0	−28.250	0.161	0.215
16	20.4	−30.533	0.094	0.139
17	21.8	−31.417	0.067	0.316
18	21.1	−33.000	0.020	0.228
19	22.0	−33.683	0.000	0.342
20	24.0	−32.367	0.039	0.595
		Zone 3		
21	27.2	−27.850	0.173	1.000
22	26.2	−24.333	0.278	0.873
23	25.3	−21.717	0.355	0.760
24	25.7	−18.700	0.445	0.810
25	25.0	−16.383	0.514	0.722
26	26.7	−12.367	0.633	0.937
27	25.8	−9.250	0.725	0.823
28	25.5	−6.433	0.809	0.785
29	25.8	−3.317	0.902	0.823
30	26.0	0.000	1.000	0.848
Max	27.2	0.000	1.000	1.000
Min	19.3	−33.683	0.000	0.000
Range	7.9	33.683		
	Zone 1	Zone 2	Zone 3	Pooled
Mean	20.07	22.06	25.92	22.68
Norm Mean	0.10	0.35	0.84	0.43
Std Dev	0.56	1.07	0.65	2.59
H	0.358	0.603	0.455	0.762

An ascending trace indicates clustering of values above the pooled mean; the larger the deviations, the steeper the slope. This relationship is clear throughout Zone 3, where average values are 25.92. In this case, the regime transition is clearly signaled by a change in the sign of the trace slope.

Note that some zone-specific values of H do not fall within the expected range of 0.5 to 1.0 due to the small sample size. The example illustrates the power of rescaling, which is robust even with small data sets. However, it emphasizes the fact that the calculation of H is best performed on long time series. Furthermore, this simple example does show all the attributes of a Hurst-Phenomenon signal produced by shifting mean zonal values. The large diameter extremes are clustered in the segment with the largest specimens (Zone 3) and the small
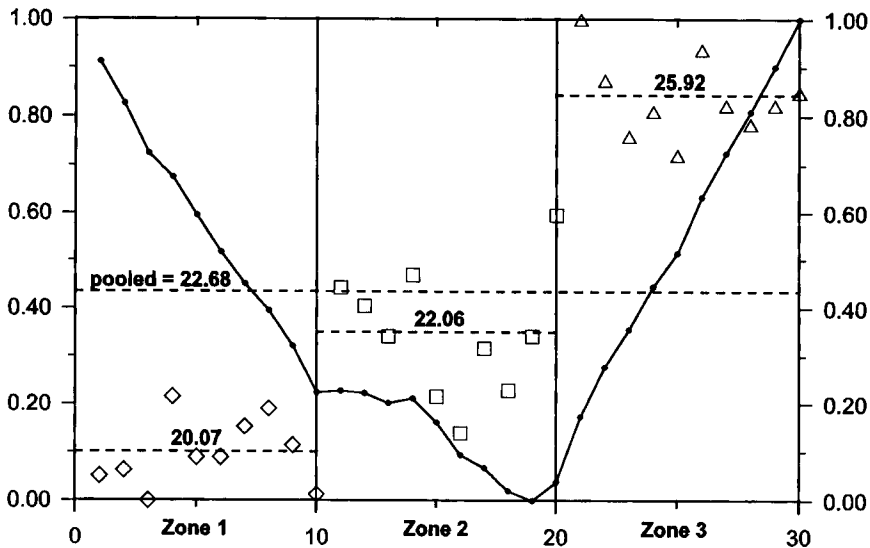
FIG. 1. Series of Tree Diameters from Three Zones, Collected along a Transect. Ten measurements were made in each zone; the mean zonal diameter is shown as a horizontal dashed line. All measurements and rescaled trace are normalized to a range of 0.0 to 1.0 (see text). Regime transitions (zonal boundaries) are shown by vertical lines.

diameter extremes cluster in the segment with the smallest mean (Zone 1). The pooled-sample value of H exhibits persistence.

In some cases, samples from a single regime (tree diameters in a zone) may have a near-Gaussian distribution. In this event, regime samples should pass the robust Kolmogorov-Smirnov (K-S) Test for a Gaussian distribution at a level which is failed by the pooled distribution (Siegel 1956). Therefore, the pooled sample would display three common attributes of the Hurst phenomenon: (1) elevated persistence indicated by a larger H than any of the component regimes (zones); (2) clustered or autocorrelated extreme events with deviations of the same sign; and (3) a more complex distribution histogram than the individual component regimes.

This simple situation can be made more realistic and germane using variable run lengths of samples from only two regimes. This effect is present in mean daily air temperatures in the American midwest during spring/autumn transitional months when either polar or tropical air masses are found in the region. Air mass transitions are rapid compared to the residence time, which typically ranges from several days to a week. Quite clearly, extreme low temperatures are associated with polar air while extreme high temperatures occur when tropical air masses invade and dominate.

Rational analysis becomes nearly impossible if the regime observations are randomly mixed, yielding short and variable run lengths. This is quite probably a feature of the Dow-Jones Industrial Average—a well-known time series governed by nonstationary processes ranging from regulatory action to "computer-automated trading." In our tree example, this would be equivalent to mixing the tree diameter measurements from all three zones and randomly drawing observations to make the calculations. The rescaled trace of this "mixed regime" would show no tendency to continually ascend or descend, but would exhibit high-frequency fluctuations.
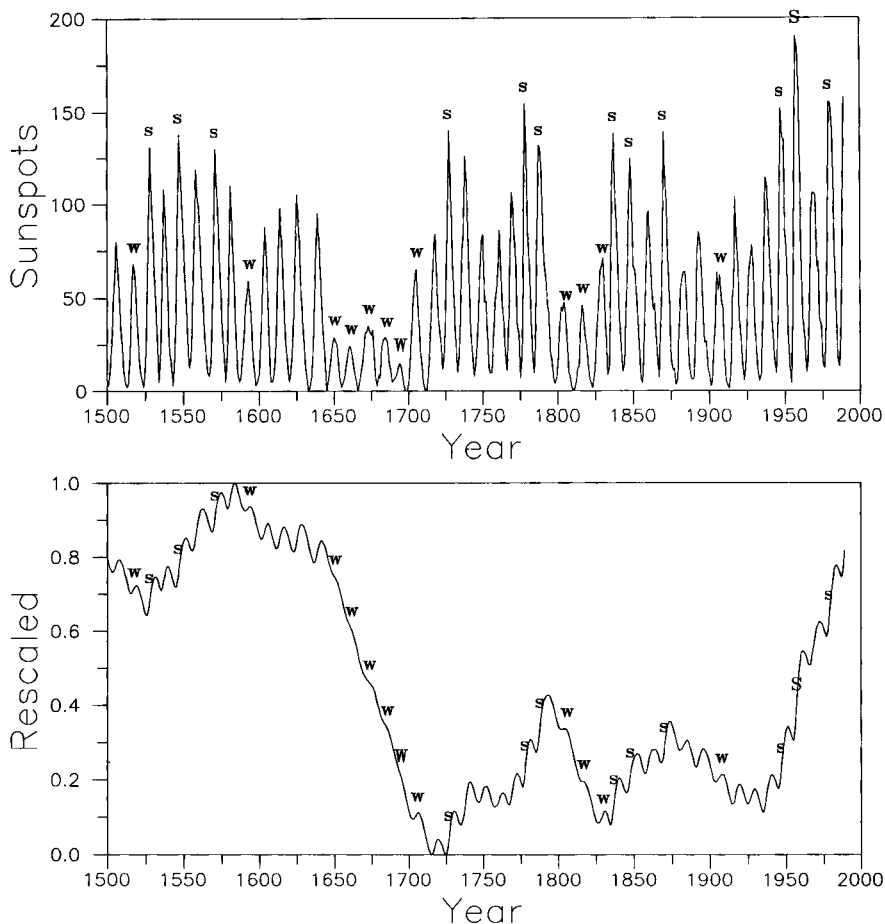
FIG. 2. Raw and Normalized (0.0–1.0) Rescaled Sunspot Numbers for Period 1500–1989. w = weak cycle, s = strong cycle.

When regime observations are not completely mixed and have variable run lengths, as in the midwest weather example, it is quite likely that the rescaled transform will signal regime transitions; these are analogous to zonal transitions. We will first examine three time series with known physical regimes to determine (1) the capacity of Hurst rescaling to signal regime transitions, and (2) the effect of Hurst regime detection on the descriptive parameters of the component regimes compared to those of the complete, or pooled, sample. Finally, a time series array with incompletely recognized physical regimes will be analyzed.

PATTERNS IN THE SUNSPOT CYCLE

To demonstrate the Hurst rescaling transformation, we will first introduce a familiar and well-documented time series. Figure 2 is a graph of sunspot numbers for the period 1500–1989, containing 490 annual observations with a mean annual value of 44.9 (Oliver and Fairbridge 1987). The 11.1-year cycle is apparent. Lower case labels on the trace indicate weak (w: <70) or strong (s: >135) cycles, as measured by the maximum annual magnitude of the cycle. The upper-

case labels indicate global extremes in the data set, with the weakest cycle peak magnitude occurring in 1694 ($W = 20$) and strongest in 1957 ($S = 194$).

The normalized rescaled time series is shown below and utilizes the same symbols. The general patterns are easy to interpret. To reiterate, an ascending trace occurs when a sequence of individual observations in the time series exceed the mean of the record, and these positive deviations are accumulated. A steep positive slope therefore indicates persistence of significantly higher-than-average values. Conversely, a trace descension results from the accumulation of observations below the record mean, and a slope near zero denotes near-average conditions over the duration. Finally, regime transitions are often signaled by a change in the sign of the trace slope.

Several patterns are apparent in the normalized rescaled sunspot number trace. First, we note that high-frequency trace fluctuations are related to the sunspot cycle, and this subcyclic information is preserved. Second, we note a slight depression in the trace centered around 1525, which corresponds to the end of the Sporer minimum (1420–1530). Following this local minimum, the trace reaches a global maximum around 1580, produced by the cumulative impact of several recurring strong cycles.

The next 150 years show a decreasing trend toward a global minimum around 1715 caused by repeating weak cycles, including the weakest cycle in 1694 (W). This is the Maunder minimum, typically dated from 1645–1715. Note, however, the duration over which the trace is declining is greater by a factor of two. Since a declining trace occurs when recurring values less than the mean of the data set are summed, the negative slope suggests a gradual reduction in sunspot activity preceding the Maunder minimum as traditionally defined, and a period of recovery extending slightly beyond the observed global minimum in 1694 (W).

The 1700s are characterized by renewed sunspot activity, with several strong cycles. This pattern is reflected as an ascension of the normalized rescaled trace which peaks locally around 1778. Three weak solar cycles in the early 1800s are followed by three strong cycles clustered in the mid-1800s. The rapid ascension near the end of the record is due to clustering of strong cycles and includes the record maximum of 1957 (S).

The calculated Hurst exponent is 0.668 for the 490-year record. If the data are first detrended, H remains the same but the rescaled trace is modified. The overall pattern is the same, with inflection points occurring at the same time. However, the trace is progressively displaced downward with time since the linear trend was positive. Thus, the global minimum on the trace occurs during the first half of the twentieth century. Since the observed trend may well be part of a longer cycle [for example, two hundred years (Schove 1983)], it is a significant part of the signal and is *not* removed from the data (Bhattacharya, Gupta, and Waymire 1983).

PRECIPITATION RECORDS AND DROUGHT

Potter (1976, 1979) used annual precipitation time series to identify nonstationarity in the record. In his studies, one hundred years of data for sites in the northeastern United States were analyzed to detect precipitation regimes and to calculate the Hurst exponent. In a similar vein, monthly precipitation amounts for the period 1948 through 1990 were obtained for five NOAA meteorological stations in the midwestern United States (NOAA 1992). This yielded 516 observations for forty-three years at each station, and includes some periods of significant drought. The normalized rescaled time series are presented as Figure 3.
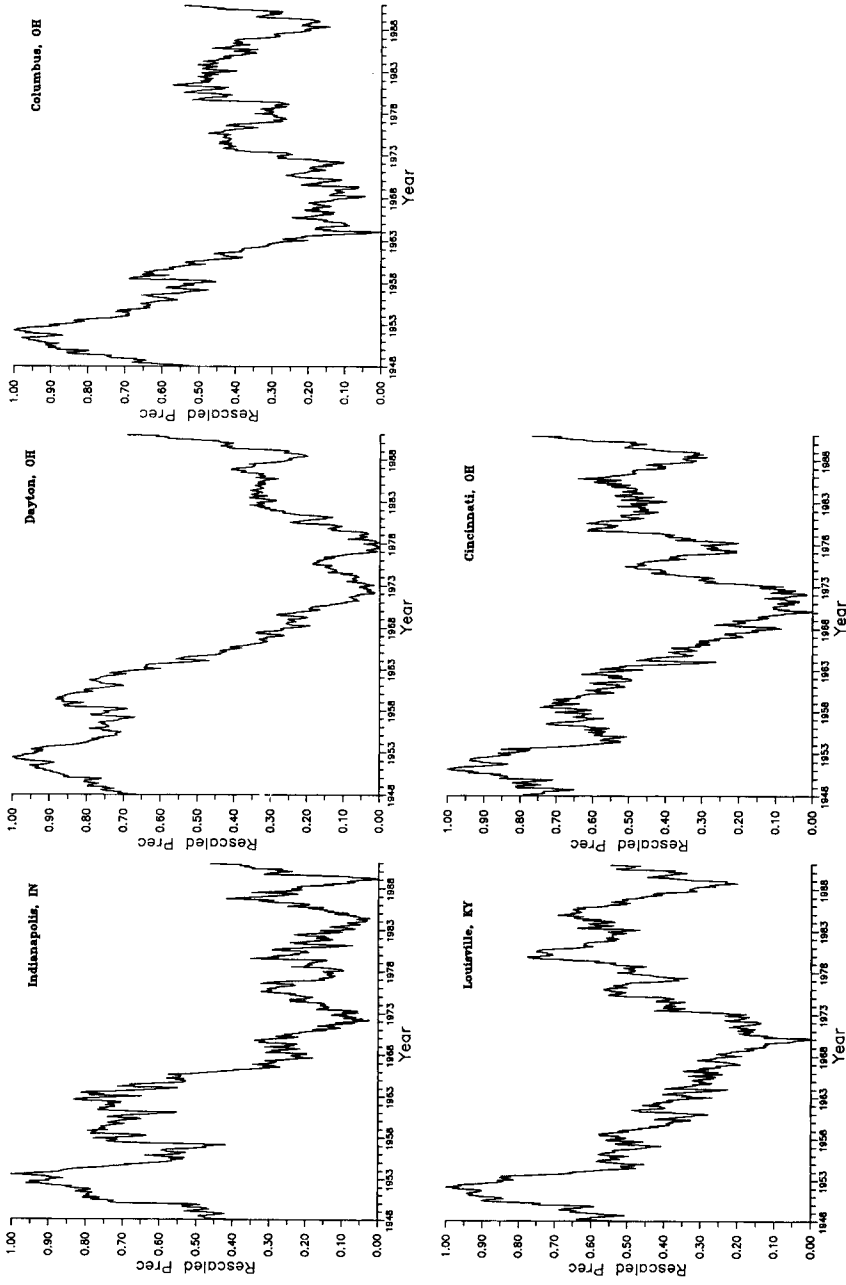
FIG. 3. Rescaled and Normalized Monthly Precipitation Data for Five Midwestern Sites, 1948–1990

TABLE 2
Summary Statistics for Monthly Precipitation, 1948–1990

Site	Mean (cm)	Max (cm)	Min (cm)	H
Indianapolis, Indiana	8.51	32.23	0.43	.532
Louisville, Kentucky	9.29	37.87	0.58	.550
Dayton, Ohio	7.77	27.66	0.43	.620
Cincinnati, Ohio	8.65	30.94	0.46	.544
Columbus, Ohio	8.01	27.10	0.28	.568

The relative station positions in Figure 3 are geographically correct; Indianapolis lies nearly due west of both Dayton and Columbus, and Cincinnati is south of Dayton. Note that the five stations represent an area extending about 250 kilometers east-west by about 100 kilometers north-south.

Summary statistics for the five sites are presented in Table 2. The largest H (0.620) is calculated for the Dayton record while Indianapolis had the smallest H of 0.532.

The traces share several common characteristics. First, note that the high-frequency variation along the trace results from seasonal precipitation fluctuations. This illustrates that short-term, high-frequency variations have minimal impact on the overall trace pattern and could be filtered for presentation. Second, note that the traces tend to peak around 1952, descend rapidly to a minimum centered around 1970, and then gradually increase again. Finally, significant depressions in the traces are centered around 1988. These patterns can be correlated to well-documented periods of drought in this region.

The traces generally ascend for the first several years of record, indicating that the individual observations in the time series exceed the mean of the record and these positive deviations are accumulated. The steep slope signifies persistence of highly abnormal observations. In this example, the ascending trace is associated with a prolonged period of greater-than-average precipitation, which peaks at a normalized rescaled value of 1.0 around 1952. For the purpose of discussion, we will call this initial regime WET1.

Following the local maxima, the traces descend rapidly toward a local minima centered around 1955, after which the traces tend to ascend temporarily. The rapid descension results from the accumulation of observations significantly below the record mean. The period 1952–1955 defines a period of drought in Ohio, which was somewhat unusual in that excessive ameliorating precipitation did not fall for the entire period. During this period, mean Palmer Hydrologic Drought Indices (PHDI) ranged from about −2.63 to −5.05 (Rogers 1993; his Fig. 3).

Although some stations indicate a return to above-normal precipitation (trace ascensions) immediately after this event, the general trend in the middle part of the record is downward. In southwestern Ohio, this culminated in a minimum normalized rescaled value of 0.0 in the mid—late 1960s. Rogers (1993) reports lowest average statewide PHDIs from −4.63 to −2.42 during this period. Although drought indices require the use of many other parameters (runoff, evapotranspiration, soil water loss and recharge, as well as potential measurements), the rescaled precipitation traces do appear to indicate both the duration and timing of these drought events. This regime will be referred to as DRY1.

A prolonged wet period occurred during the period 1966–1987 across this region, and is reflected as a gradual ascension of the traces. This pattern is interrupted in the late 1970s and 1980s by short dry spells (PHDI of −3.06

TABLE 3
Precipitation Regime Summary Statistics, Columbus, Ohio

Regime (Month)	H	Mean (Std Dev)	K-S/Gauss (P10%)
WET1 (0-52)	0.520	9.34 (4.10)	0.047/0.157=0.280
DRY1 (52-193)	0.540	6.96 (4.10)	0.074/0.102=0.725
WET2 (193-515)	0.516	8.26 (4.50)	0.063/0.068=0.926
Pooled (0-515)	0.568	8.01 (4.42)	0.066/0.054=1.222*

* distribution not Gaussian at the 10 percent level

during the growing season of 1988), but the end of all records show a rapid ascension and return to above-normal precipitation conditions. Although clearly interrupted by dry periods, we will refer to this regime as WET2.

Having defined three general regimes, with boundaries delimited by significant trace inflections where the slope changes sign, we will use the Columbus, Ohio, time series to illustrate the statistical analysis of the regimes. The Hurst exponent is calculated individually for each of the three regimes as delimited by trace inflections. WET1 extends from month 0 to 52, as a maximum rescaled value of 1.0 occurs at observation 52 in the Columbus time series. DRY1 runs from month 52 to 193, when a normalized rescaled value of 0.0 is encountered. WET2 extends from this global minima to the end of the record (193–515). H for each regime is reported in Table 3, along with the mean and standard deviation of that raw record segment. In addition, the Kolmogorov-Smirnov (K-S) and Gaussian statistics, calculated at the 10 percent significance level, are reported. If the K-S statistic is less than the Gaussian statistic, the distribution is normal at the 10 percent level. Thus, the K-S/Gauss ratio of > 1.00 indicates a non-Gaussian distribution.

From Table 3, each precipitation regime K-S/Gauss ratio is less than unity, indicating a normal distribution. However, the pooled data are distinctly non-normal. Thus, crudely dividing the time series into three regimes indicates non-stationarity in the data set. Furthermore, we note that the pooled H exceeds that calculated for any single regime. This record therefore exhibits all the characteristics of a "three-tree zone" system as outlined in the introduction, and the rescaled traces are used to discriminate between regimes of fundamentally different character.

It should be stressed that there is no physical reason that component regimes of all geophysical systems should display near-Gaussian distributions. Of the five stations analyzed here, Louisville and Dayton had statistical results similar to the Columbus station. Conversely, Indianapolis and Cincinnati had one regime with a non-Gaussian distribution. It is interesting to note that these two stations also had the lowest pooled H (Table 2).

In summary, Hurst rescaling of monthly precipitation serial data defines regimes which were more Gaussian and less persistent than the pooled data. These findings are consistent with the conceptual model.

ARIZONA WATERSHED DISCHARGE

The annual inflow, or watershed discharge, into the Horseshoe and Roosevelt Reservoirs in central Arizona for the period 1914–1992 were normalized and rescaled, and are plotted as Figure 4. The rescaled maximum, minimum, and a prominent inflection in 1941 divided both sets of data into four regimes. It is interesting to note that the data share two common transition points marked
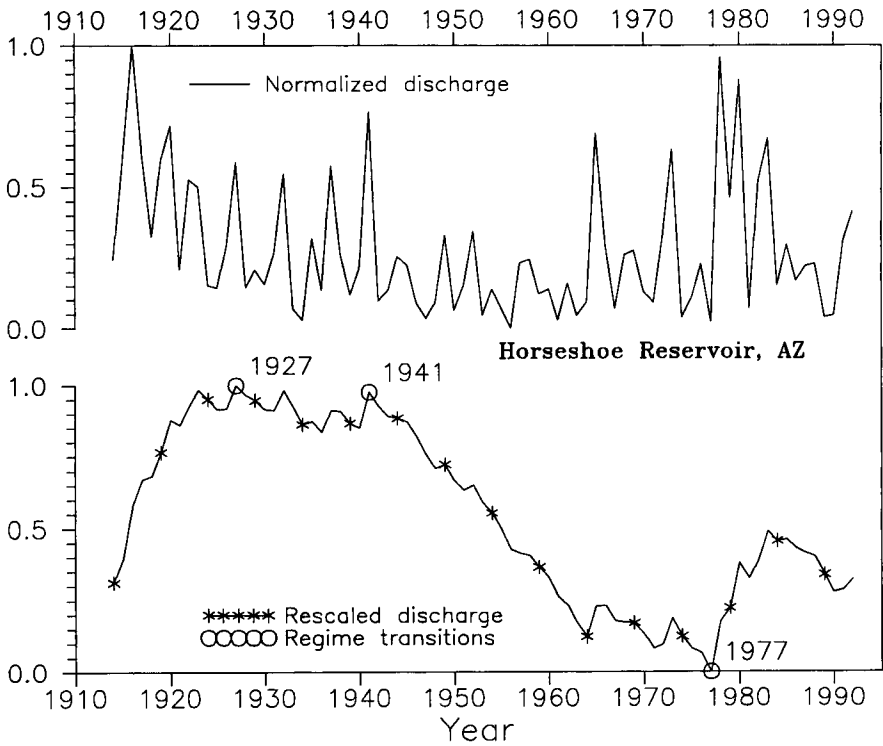
FIG. 4a. Normalized Annual Raw and Rescaled Discharge into Horseshoe Reservoir. Trace inflections (circles) signal regime transitions.
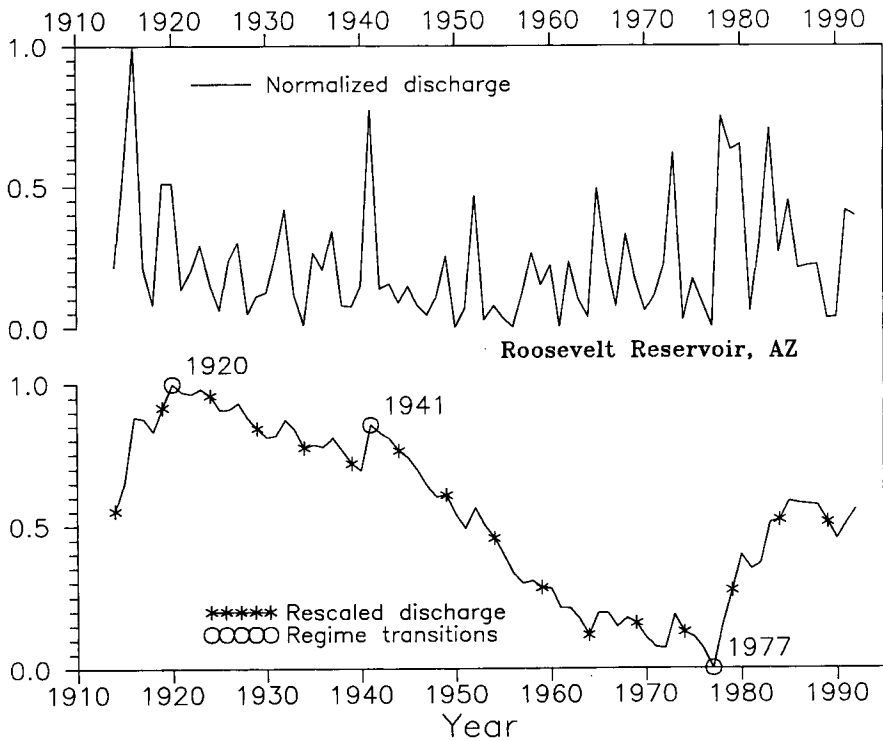

FIG. 4b. Normalized Annual Raw and Rescaled Discharge into Roosevelt Reservoir

TABLE 4
Statistics for Annual Reservoir Inflow Regimes

Record	H	Mean (Std Dev)	K-S/Gauss (P20%)
Horseshoe			
1914–1927	0.567	0.46(0.24)	0.107/0.274=0.391
1927–1941	0.472	0.29(0.21)	0.167/0.266=0.628
1941–1977	0.541	0.19(0.18)	0.122/0.176=0.693
1977–1992	0.605	0.34(0.28)	0.125/0.258=0.484
1914–1992	0.640	0.28(0.24)	0.146/0.120=1.217*
Roosevelt			
1914–1920	0.449	0.44(0.29)	0.179/0.381=0.470
1920–1941	0.515	0.22(0.17)	0.091/0.233=0.391
1941–1977	0.498	0.17(0.17)	0.149/0.176=0.847
1977–1992	0.561	0.33(0.24)	0.063/0.258=0.244
1914–1992	0.636	0.23(0.21)	0.146/0.120=1.217*

* distribution not Gaussian at 20 percent level

by the 1977 minimum and the 1941 inflection point. The statistical parameters for these regimes at two locations are presented as Table 4.

Independent analyses of central Arizona climate from the turn of the century to the near-present suggest significant regional wet periods (more than ten months duration) in 1915–17, 1919–20, 1931–33, 1940–41, 1965–66, 1972–73, and 1978–80. Throughout the 1920s and 1930s, near-average precipitation yields a rescaled discharge trace that does not change much during this period. The 1941 inflection point divides a prolonged subsequent dry period from the preceding long-duration period of average precipitation. The 1977 inflection ends this post-1941 dry segment in the record, and signals commencement of a wetter phase extending from 1977 to the present (Brazel 1986; Eychaner, Rehmann, and Brazel 1989). Again, the identified regimes show decreased persistence and are more Gaussian than the pooled record.

THERMAL REGIME TRANSITION DETECTION IN SOIL ABOVE PERMAFROST

In this final example, we will explore the correlation between rescaled extremes and inflections using a two-dimensional array of soil temperatures. Rescaled traces will be used to identify transitions between thermal regimes characterized by differing modes of heat transfer. This example therefore provides the link between the detected regimes and the underlying physical processes.

The *active layer* is the zone of summer thaw and winter refreezing above permafrost, or permanently frozen ground. Hourly temperature measurements were made at eight probes buried in the upper soil at a site near Fairbanks, Alaska, extending from mid-August 1992 to mid-August 1993. The probes are vertically spaced at seven-centimeter intervals beginning one centimeter below the surface. Thus, the lowest (eighth) probe is at fifty centimeters, near the base of the active layer. The mean daily temperatures for the 363-day period at the upper probe is displayed in Figure 5.

Three thermal regimes are generally discernible in the annual cycle. The active layer (AL) regime develops in summer, when the thawed zone is deepening. This is a period when conduction tends to dominate, but nonconductive heat transfer processes significantly affect the thermal evolution of the active layer. Precipitation infiltration and soil water evaporation, for example, are particularly important during this period (Hinkel and Outcalt 1994).
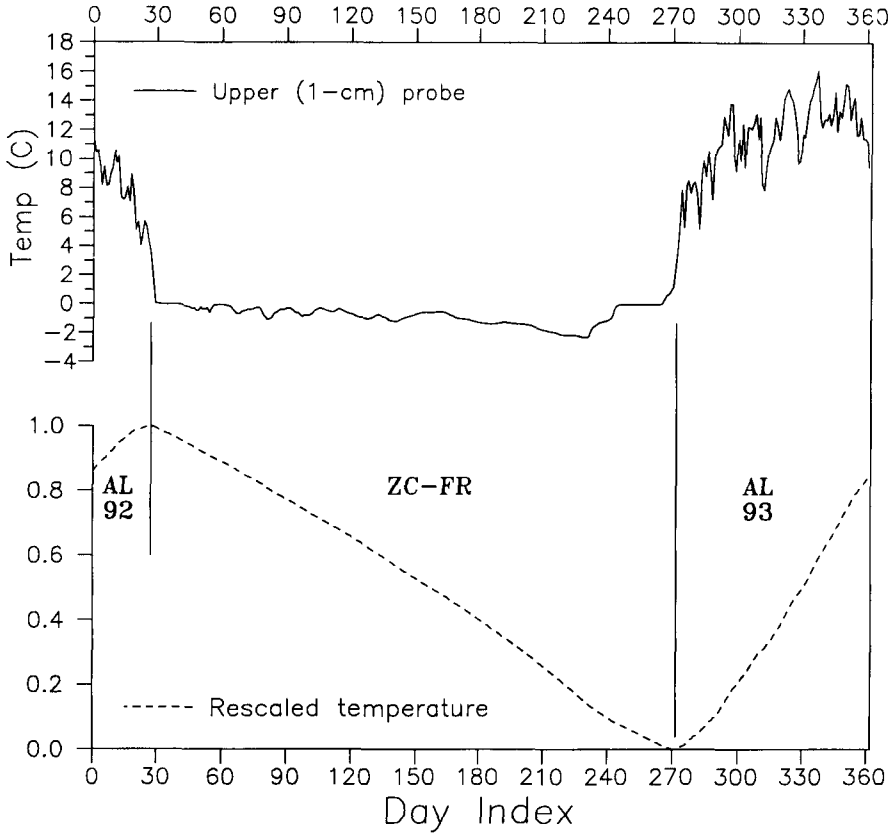
FIG. 5. Mean Daily and Rescaled Temperature from Near-Surface Probe for Period Mid-August 1992 to Mid-August 1993. AL = active layer regime; ZC = zero curtain regime; FR = freezing regime.

As the active layer refreezes from the surface downward in autumn and early winter, temperatures in the lower part of the active layer are isothermal near 0°C, often for several months. This is known as the *zero-curtain effect* (Sumgin et al. 1940), and this period is referred to as the zero curtain (ZC) regime. Although heat conduction cannot occur across an isothermal zone, water and water vapor migrate vertically across the unfrozen layer in response to osmotic gradients, transporting both sensible and latent heat upward. This regime is therefore dominated by nonconductive heat transfer effects (Outcalt, Nelson, and Hinkel 1990).

In mid—late winter, as subfreezing temperatures penetrate to depth, the active layer freezes and the freezing (FR) regime commences. Once the pathways between soil pores become blocked with ice, the movement of water and water vapor is restricted and conduction dominates. This regime is truncated with spring thaw and the AL regime begins the cycle again.

These divisions are based on the dominant heat transfer process, so the regime patterns are known from other analyses (Outcalt, Nelson, and Hinkel 1990; Hinkel and Outcalt 1994, 1995). Regime transitions, however, are not easily discriminated. The statistics for the three regimes identified by rescaling are reported in Table 5.

TABLE 5
Regime Statistical Summary for Mean Daily Temperature at One-Centimeter Depth

Regime (Days)	H	Mean (Std Dev)	K-S/Gauss (P10%)
AL92 (0-31)	0.744	6.84 (3.16)	0.125/0.216=0.579
ZC-FR (31-266)	0.823	−0.81 (0.61)	0.064/0.079=0.810
AL93 (266-362)	0.760	10.80 (3.50)	0.119/0.124=0.960
Pooled (0-362)	0.863	2.96 (5.60)	0.172/0.064=2.87*

* distribution not Gaussian at the 10 percent level

We note that each of the regimes is both less persistent and more Gaussian than the pooled data. Furthermore, we note that Hurst rescaling of the one-centimeter data only detects the transitions between the summer 1992 thaw (AL92), the composite winter regime (ZC-FR), and the 1993 thaw (AL93). Thus, using only data from the upper probe, we are unable to differentiate between the ZC and FR regimes. This is not surprising given that soil regimes characterize a *region* of the soil; temperature at a single probe level simply cannot capture depth-dependent variations.

For this reason, all eight probes were analyzed to exploit the full richness of the data array. These raw data and their normalized rescaled transforms are plotted as Figure 6. Rescaled trace extremes and inflections, occurring at nearly the same time in the soil column, clearly define the AL92-ZC and ZC-FR regime boundaries. Furthermore, the analysis reveals a previously unidentified regime. Spring warming of the active layer occurs quite suddenly around Day Index 240 (mid-May). This event is associated with snow melt and downward movement of meltwater into the active layer. Lasting about thirty days, this is referred to as the snow melt (SM) regime as warming is largely accomplished by nonconductive transfer of both mass and heat from above.

The thermal regimes of the lower six probes have non-Gaussian distributions. This analysis demonstrates the regime transition-detection power of Hurst rescaling; in fact, the snow melt (SM) regime was first identified using the technique.

CONCLUSIONS

Empirical investigation of sunspot numbers, precipitation, hydrological, and shallow geothermal temperature time series supports the general view that the Hurst phenomenon might be produced by mixing distinct physical regimes. The component regimes often have significantly different descriptive parameters than the serial data from which they were extracted. These empirical observations fit the conceptual model of enhanced persistence traceable to regime mixing.

The nonstationary model used here is similar to that proposed by Klemes (1974) and Potter (1976), but other explanations of the Hurst phenomenon have been proposed and formalized. Our emphasis has been on the interpretation of inflections and extremes on the normalized rescaled trace.

Hurst rescaling provides a simple method of screening serial geophysical data for natural regime transitions and data acquisition artifacts. Inflections on the rescaled trace mark the regime boundaries and isolate a segment of the time series containing a trace that either ascends, descends, or remains nearly constant. A positive trace slope indicates temporal persistence of above-normal measurements, while a negative trace slope reflects persistence of observations below the record mean. Furthermore, a steeper slope indicates temporal clus-
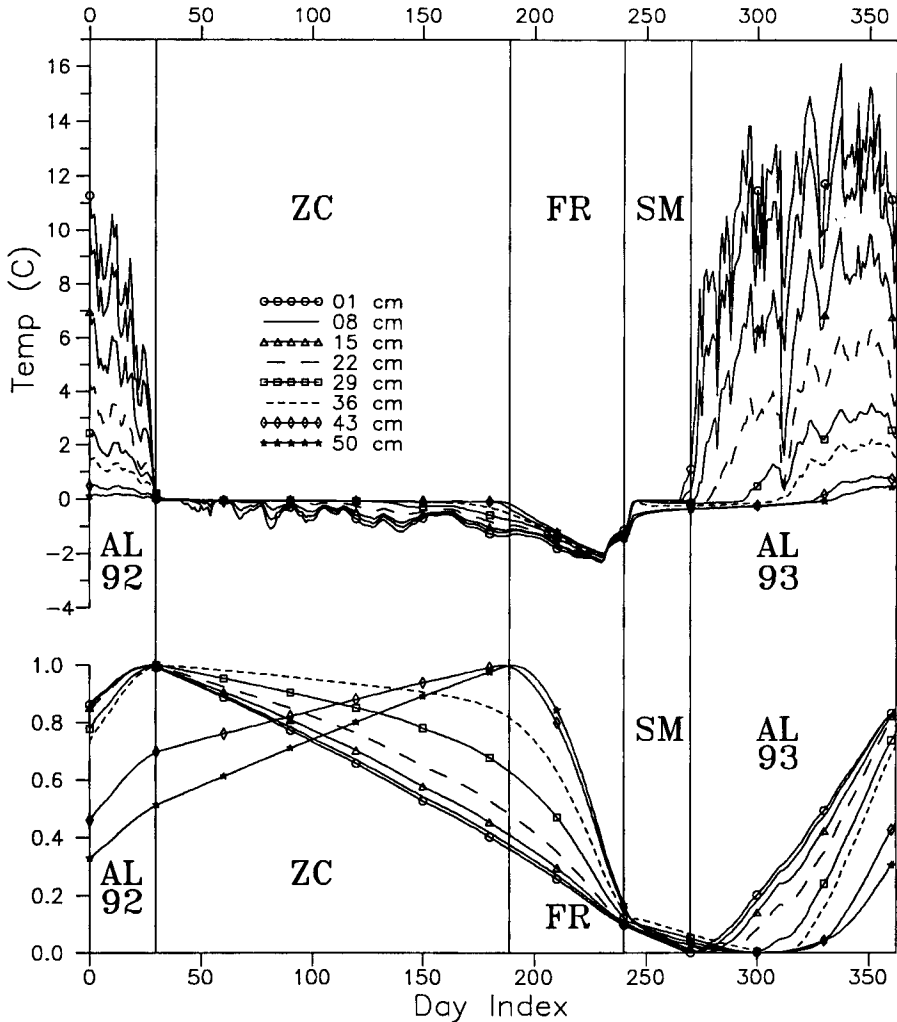
FIG. 6. Mean Daily and Rescaled Temperature for an Eight-Probe Array in the Active Layer above Permafrost. Upper probes traces are warmer in summer and colder in winter. SM = snow melt regime.

tering of similar extreme events. The regimes detected by Hurst rescaling can be correlated to well-documented phases and, by analogy, could also be to used to analyze tree-growth rings, mud varve thickness, and time series of atmospheric pressure. At a practical level, the method can be used to "formalize" the transitions between natural regimes with no reference to the Hurst phenomenon. Analysis of temperature time series from eight levels in the upper soil profile supports the view that several thermal regimes develop during the annual cycle, and that each regime is uniquely associated with a characteristic set of conductive and nonconductive heat transfer processes.

Since the rescaled range tends to increase with the number of observations, it is likely that the Hurst rescaling transform method is only effective in identifying regime shifts when regime species have sufficient run lengths. Temporal autocorrelation of geophysical serial data yields relatively long runs, the data

attribute that makes regime transitions detectable at a site. Complete regime mixing is not probable in climate-governed geophysical time series as the global fluid systems have strong persistence. This nearly universal species persistence is an attribute of geophysical systems that makes regime identification tractable at a site. This is a general attribute of hydro-climatological serial data that is forced, to a large extent, by circulation pattern transitions in the large fluid systems of the atmosphere and oceans.

LITERATURE CITED

Bhattacharya, R. N., V. K. Gupta, and E. Waymire (1983). "The Hurst Effect under Trends." *Journal of Applied Probability* 20, 649–62.

Boes, D. C., and J. D. Salas (1978). "Nonstationarity of the Mean and the Hurst Phenomenon." *Water Resources Research* 14(1), 135–43.

Brazel, A. J. (1986). "Statewide Temperature and Moisture Trends, 1895–1983." In *Arizona Climate: The First Hundred Years*, edited by W. D. Sellers, R. H. Hill, and M. Sanderson-Rae, pp. 79–84. Tuscon: University of Arizona Press.

Church, M. (1980). "Records of Recent Geomorphological Events." In *Timescales in Geomorphology*, edited by R. A. Cullingform, D. A. Davidson, and J. Lewin, pp. 13–29. New York: John Wiley and Sons.

Eychaner, J. H., M. R. Rehmann, and A. J. Brazel (1989). "Arizona Floods and Droughts." *Floods and Droughts, State Summaries*. National Water Summary, 1988–89. USGS Water Supply Paper 2375, pp. 181–88.

Hinkel, K. M., and S. I. Outcalt (1994). "Identification of Heat Transfer Processes during Soil Cooling, Freezing, and Thaw in Central Alaska." *Permafrost and Periglacial Processes* 5(4), 217–35.

——— (1995). "The Detection of Heat-Mass Transfer Regime Transitions in the Active Layer Using Fractal Geometry." *Cold Regions Science and Technology* 23, 293–304.

Hurst, H. E. (1951). "Long-Term Storage Capacity of Reservoirs." *Transactions of the American Society of Civil Engineers* 116, 770–99.

Hurst, H. E., R. P. Black, and Y. M. Simaika (1965). *Long-Term Storage: An Experimental Study*. London: Constable Press.

Klemes, V. (1974). "The Hurst Phenomenon: A Puzzle?" *Water Resources Research* 10(4), 675–88.

Mandelbrot, B. B. (1982). *The Fractal Geometry of Nature*. New York: W.H. Freeman and Co.

Mandelbrot, B. B., and J. Wallis (1969). "Robustness of the Rescaled Range R/S in the Measurement of Noncyclic Long-Run Statistical Dependence." *Water Resources Research* 5(5), 967–88.

Mesa, O. J., and G. Poveda (1993). "The Hurst Effect: The Scale of Fluctuation Approach." *Water Resources Research* 29(12), 3995–4002.

NOAA (1992). *International Station Meteorological Climate Summary*. CD-ROM Version 2.0. Asheville, N.C.: Federal Climate Complex.

Oliver, J. E., and R. W. Fairbridge, eds. (1987). *The Encyclopedia of Climatology*. New York: Van Nostrand Reinhold.

Outcalt, S. I., F. E. Nelson, and K. M. Hinkel (1990). "The Zero-Curtain Effect: Heat and Mass Transfer across an Isothermal Region in Freezing Soil." *Water Resources Research* 26(7), 1509–16.

Potter, K. W. (1976). "Evidence for Nonstationarity as a Physical Explanation of the Hurst Phenomenon." *Water Resources Research* 12(15), 1047–52.

——— (1979). "Annual Precipitation in the Northeast United States: Long Memory, Short Memory, or No Memory?" *Water Resources Research* 15(2), 340–46.

Rogers, J. C. (1993). "Climatological Aspects of Drought in Ohio." *Ohio Journal of Science* 93(3), 51–59.

Schove, D. J., ed. (1983). *Sunspot Cycles*. Benchmark Papers in Geology, vol. 68, Stroudsburg, Penn.: Hutchinson Ross.

Schroeder, M. (1991). *Fractals, Chaos, Power Laws: Minutes from an Infinite Paradise*. New York: W.H. Freeman and Co.

Siegel, S. (1956). *Nonparametric Statistics for the Behavioral Sciences*. New York: McGraw-Hill.

Stolum, H.-H. (1996). "River Meandering as a Self-Organization Process." *Science* (271), 1710–13.

Sumgin, M. I., S. P. Kachurin, N. I. Tolstikhin, and V. F. Tumel' (1940). *Obshchee Merzlotovedenie [General Permafrostology]*. Moscow: Academiia Nauk SSR.

Wallis, J. R., and P. E. O'Connell (1973). "Firm Reservoir Yield—How Reliable Are Historic Hydrological Records?" *Hydrological Science Bulletin* 18(3), 347–65.